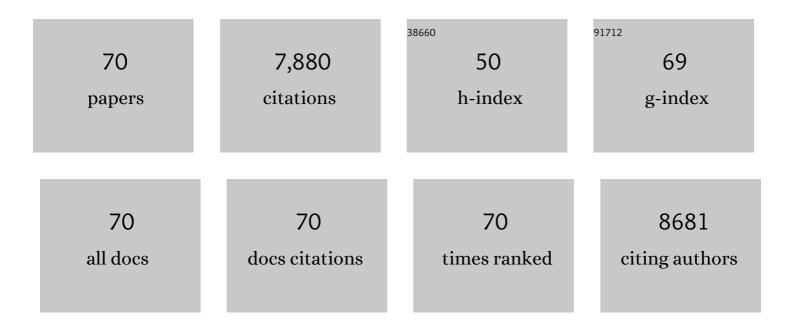
List of Publications by Year in descending order

Source: https://exaly.com/author-pdf/9011586/publications.pdf Version: 2024-02-01



#	Article	IF	CITATIONS
1	MoS ₂ Quantum Dot Growth Induced by S Vacancies in a ZnIn ₂ S ₄ Monolayer: Atomic-Level Heterostructure for Photocatalytic Hydrogen Production. ACS Nano, 2018, 12, 751-758.	7.3	500
2	Ag3PO4/Ti3C2 MXene interface materials as a Schottky catalyst with enhanced photocatalytic activities and anti-photocorrosion performance. Applied Catalysis B: Environmental, 2018, 239, 545-554.	10.8	481
3	Vertical single or few-layer MoS2 nanosheets rooting into TiO2 nanofibers for highly efficient photocatalytic hydrogen evolution. Applied Catalysis B: Environmental, 2015, 164, 1-9.	10.8	465
4	Atomic scale g-C3N4/Bi2WO6 2D/2D heterojunction with enhanced photocatalytic degradation of ibuprofen under visible light irradiation. Applied Catalysis B: Environmental, 2017, 209, 285-294.	10.8	390
5	0D/2D interface engineering of carbon quantum dots modified Bi2WO6 ultrathin nanosheets with enhanced photoactivity for full spectrum light utilization and mechanism insight. Applied Catalysis B: Environmental, 2018, 222, 115-123.	10.8	288
6	Scalable one-step production of porous oxygen-doped g-C3N4 nanorods with effective electron separation for excellent visible-light photocatalytic activity. Applied Catalysis B: Environmental, 2018, 224, 1-9.	10.8	269
7	Selfâ€Optimization of the Active Site of Molybdenum Disulfide by an Irreversible Phase Transition during Photocatalytic Hydrogen Evolution. Angewandte Chemie - International Edition, 2017, 56, 7610-7614.	7.2	221
8	Engineering MoS2 nanomesh with holes and lattice defects for highly active hydrogen evolution reaction. Applied Catalysis B: Environmental, 2018, 239, 537-544.	10.8	219
9	Nature of extra capacity in MoS2 electrodes: Molybdenum atoms accommodate with lithium. Energy Storage Materials, 2019, 16, 37-45.	9.5	218
10	Positioning cyanamide defects in g-C3N4: Engineering energy levels and active sites for superior photocatalytic hydrogen evolution. Applied Catalysis B: Environmental, 2018, 237, 24-31.	10.8	207
11	<i>In Situ</i> Alloying Strategy for Exceptional Potassium Ion Batteries. ACS Nano, 2019, 13, 3703-3713.	7.3	194
12	Photocatalytic wastewater purification with simultaneous hydrogen production using MoS 2 QD-decorated hierarchical assembly of ZnIn 2 S 4 on reduced graphene oxide photocatalyst. Water Research, 2017, 121, 11-19.	5.3	176
13	Ultrastable Potassium Storage Performance Realized by Highly Effective Solid Electrolyte Interphase Layer. Small, 2018, 14, e1801806.	5.2	175
14	Silver phosphate-based Z-Scheme photocatalytic system with superior sunlight photocatalytic activities and anti-photocorrosion performance. Applied Catalysis B: Environmental, 2017, 208, 1-13.	10.8	174
15	Facile fabrication of mediator-free Z-scheme photocatalyst of phosphorous-doped ultrathin graphitic carbon nitride nanosheets and bismuth vanadate composites with enhanced tetracycline degradation under visible light. Journal of Colloid and Interface Science, 2018, 509, 219-234.	5.0	160
16	WS2 moirel•superlattices derived from mechanical flexibility for hydrogen evolution reaction. Nature Communications, 2021, 12, 5070.	5.8	152
17	Monolayer MoS ₂ with S vacancies from interlayer spacing expanded counterparts for highly efficient electrochemical hydrogen production. Journal of Materials Chemistry A, 2016, 4, 16524-16530.	5.2	148
18	Glucose-assisted synthesize 1D/2D nearly vertical CdS/MoS 2 heterostructures for efficient photocatalytic hydrogen evolution. Chemical Engineering Journal, 2017, 321, 366-374.	6.6	135

#	Article	IF	CITATIONS
19	Photoinduced semiconductor-metal transition in ultrathin troilite FeS nanosheets to trigger efficient hydrogen evolution. Nature Communications, 2019, 10, 399.	5.8	133
20	A promising inorganic-organic Z-scheme photocatalyst Ag3PO4/PDI supermolecule with enhanced photoactivity and photostability for environmental remediation. Applied Catalysis B: Environmental, 2020, 263, 118327.	10.8	129
21	A multifunctional platform by controlling of carbon nitride in the core-shell structure: From design to construction, and catalysis applications. Applied Catalysis B: Environmental, 2019, 258, 117957.	10.8	126
22	A novel aluminum dual-ion battery. Energy Storage Materials, 2018, 11, 91-99.	9.5	123
23	Boosting Photocatalytic Performance in Mixed-Valence MIL-53(Fe) by Changing Fe ^{II} /Fe ^{III} Ratio. ACS Applied Materials & Interfaces, 2019, 11, 28791-28800.	4.0	121
24	Omnidirectional enhancement of photocatalytic hydrogen evolution over hierarchical "cauline leaf― nanoarchitectures. Applied Catalysis B: Environmental, 2016, 186, 88-96.	10.8	117
25	A three-dimensional graphitic carbon nitride belt network for enhanced visible light photocatalytic hydrogen evolution. Journal of Materials Chemistry A, 2016, 4, 19003-19010.	5.2	111
26	Sea-urchin-structure g-C3N4 with narrow bandgap (˜2.0 eV) for efficient overall water splitting under visible light irradiation. Applied Catalysis B: Environmental, 2019, 249, 275-281.	10.8	110
27	1T-MoS2 nanosheets confined among TiO2 nanotube arrays for high performance supercapacitor. Chemical Engineering Journal, 2019, 366, 163-171.	6.6	105
28	Facile synthesis of bismuth oxyhalogen-based Z-scheme photocatalyst for visible-light-driven pollutant removal: Kinetics, degradation pathways and mechanism. Journal of Cleaner Production, 2019, 225, 898-912.	4.6	101
29	Recent advances in two-dimensional nanomaterials for photocatalytic reduction of CO ₂ : insights into performance, theories and perspective. Journal of Materials Chemistry A, 2020, 8, 19156-19195.	5.2	101
30	In-situ hydrogenation engineering of ZnIn2S4 for promoted visible-light water splitting. Applied Catalysis B: Environmental, 2019, 241, 483-490.	10.8	98
31	Visible-light photocatalytic degradation of multiple antibiotics by AgI nanoparticle-sensitized Bi5O7I microspheres: Enhanced interfacial charge transfer based on Z-scheme heterojunctions. Journal of Catalysis, 2017, 352, 160-170.	3.1	92
32	A bamboo-inspired hierarchical nanoarchitecture of Ag/CuO/TiO2 nanotube array for highly photocatalytic degradation of 2,4-dinitrophenol. Journal of Hazardous Materials, 2016, 313, 244-252.	6.5	89
33	Cracked monolayer 1T MoS ₂ with abundant active sites for enhanced electrocatalytic hydrogen evolution. Catalysis Science and Technology, 2017, 7, 718-724.	2.1	83
34	Tailoring activation sites of metastable distorted 1T′-phase MoS2 by Ni doping for enhanced hydrogen evolution. Nano Research, 2022, 15, 5946-5952.	5.8	80
35	The individual and Co-exposure degradation of benzophenone derivatives by UV/H2O2 and UV/PDS in different water matrices. Water Research, 2019, 159, 102-110.	5.3	79
36	Boosted photogenerated carriers separation in Z-scheme Cu3P/ZnIn2S4 heterojunction photocatalyst for highly efficient H2 evolution under visible light. International Journal of Hydrogen Energy, 2020, 45, 14334-14346.	3.8	78

#	Article	IF	CITATIONS
37	Semimetallic vanadium molybdenum sulfide for high-performance battery electrodes. Journal of Materials Chemistry A, 2018, 6, 9411-9419.	5.2	73
38	Low-temperature synthesis of edge-rich graphene paper for high-performance aluminum batteries. Energy Storage Materials, 2018, 15, 361-367.	9.5	73
39	An artificial organic-inorganic Z-scheme photocatalyst WO3@Cu@PDI supramolecular with excellent visible light absorption and photocatalytic activity. Chemical Engineering Journal, 2020, 381, 122691.	6.6	72
40	Dislocation-strained MoS2 nanosheets for high-efficiency hydrogen evolution reaction. Nano Research, 2022, 15, 4996-5003.	5.8	72
41	Fe1-xZnxS ternary solid solution as an efficient Fenton-like catalyst for ultrafast degradation of phenol. Journal of Hazardous Materials, 2018, 353, 393-400.	6.5	62
42	Accessible COF-Based Functional Materials for Potassium-Ion Batteries and Aluminum Batteries. ACS Applied Materials & Interfaces, 2019, 11, 44352-44359.	4.0	62
43	Ingeniously designed Ni-Mo-S/ZnIn2S4 composite for multi-photocatalytic reaction systems. Chinese Chemical Letters, 2022, 33, 1468-1474.	4.8	62
44	Selfâ€Optimization of the Active Site of Molybdenum Disulfide by an Irreversible Phase Transition during Photocatalytic Hydrogen Evolution. Angewandte Chemie, 2017, 129, 7718-7722.	1.6	61
45	"Dark Deposition―of Ag Nanoparticles on TiO ₂ : Improvement of Electron Storage Capacity To Boost "Memory Catalysis―Activity. ACS Applied Materials & Interfaces, 2018, 10, 25350-25359.	4.0	61
46	Nature of Bimetallic Oxide Sb ₂ MoO ₆ /rGO Anode for Highâ€Performance Potassiumâ€Ion Batteries. Advanced Science, 2019, 6, 1900904.	5.6	60
47	Vertically Aligned Ultrathin 1T-WS2 Nanosheets Enhanced the Electrocatalytic Hydrogen Evolution. Nanoscale Research Letters, 2018, 13, 167.	3.1	57
48	Formation of Mo2C/hollow tubular g-C3N4 hybrids with favorable charge transfer channels for excellent visible-light-photocatalytic performance. Applied Surface Science, 2020, 527, 146757.	3.1	56
49	Atomicâ€Level Design of Active Site on Twoâ€Dimensional MoS ₂ toward Efficient Hydrogen Evolution: Experiment, Theory, and Artificial Intelligence Modelling. Advanced Functional Materials, 2022, 32, .	7.8	53
50	β-FeOOH on carbon nanotubes as a cathode material for Na-ion batteries. Energy Storage Materials, 2017, 8, 147-152.	9.5	52
51	Cu-Doped Fe@Fe ₂ O ₃ core–shell nanoparticle shifted oxygen reduction pathway for high-efficiency arsenic removal in smelting wastewater. Environmental Science: Nano, 2018, 5, 1595-1607.	2.2	52
52	Oriented facet heterojunctions on CdS nanowires with high photoactivity and photostability for water splitting. Applied Catalysis B: Environmental, 2020, 268, 118744.	10.8	52
53	Facile synthesis of bird's nest-like TiO2 microstructure with exposed (001) facets for photocatalytic degradation of methylene blue. Applied Surface Science, 2017, 391, 228-235.	3.1	50
54	Popcorn balls-like ZnFe 2 O 4 -ZrO 2 microsphere for photocatalytic degradation of 2,4-dinitrophenol. Applied Surface Science, 2017, 407, 470-478.	3.1	47

#	Article	IF	CITATIONS
55	Ultrafine Ag@AgI nanoparticles on cube single-crystal Ag3PO4 (1 0 0): An all-day-active Z-Scheme photocatalyst for environmental purification. Journal of Colloid and Interface Science, 2019, 533, 95-105.	5.0	44
56	Extra lithium-ion storage capacity enabled by liquid-phase exfoliated indium selenide nanosheets conductive network. Energy and Environmental Science, 2020, 13, 2124-2133.	15.6	35
57	Hierarchical Heterostructure of ZnO@TiO2 Hollow Spheres for Highly Efficient Photocatalytic Hydrogen Evolution. Nanoscale Research Letters, 2017, 12, 531.	3.1	33
58	Hierarchical architectures of ZnS–In2S3 solid solution onto TiO2 nanofibers with high visible-light photocatalytic activity. Journal of Alloys and Compounds, 2015, 624, 44-52.	2.8	31
59	Amorphous molybdenum sulfide and its Mo-S motifs: Structural characteristics, synthetic strategies, and comprehensive applications. Nano Research, 2022, 15, 8613-8635.	5.8	28
60	Atom elimination strategy for MoS2 nanosheets to enhance photocatalytic hydrogen evolution. Chinese Chemical Letters, 2023, 34, 107489.	4.8	26
61	CdSâ€Nanoparticlesâ€Decorated Perpendicular Hybrid of MoS ₂ and Nâ€Doped Graphene Nanosheets for Omnidirectional Enhancement of Photocatalytic Hydrogen Evolution. ChemCatChem, 2016, 8, 2557-2564.	1.8	25
62	In-situ potentiostatic activation to optimize electrodeposited cobalt-phosphide electrocatalyst for highly efficient hydrogen evolution in alkaline media. Chemical Physics Letters, 2017, 681, 90-94.	1.2	22
63	Revisiting lithium-storage mechanisms of molybdenum disulfide. Chinese Chemical Letters, 2022, 33, 1779-1797.	4.8	21
64	Three-dimensional reduced graphene oxide–Mn 3 O 4 nanosheet hybrid decorated with palladium nanoparticles for highly efficient hydrogen evolution. International Journal of Hydrogen Energy, 2018, 43, 3369-3377.	3.8	18
65	Ultrathin Honeycomb-like Carbon as Sulfur Host Cathode for High Performance Lithium–Sulfur Batteries. ACS Applied Energy Materials, 2018, 1, 7076-7084.	2.5	17
66	Hollow Microsphere TiO ₂ /ZnO p–n Heterojuction with High Photocatalytic Performance for 2,4-Dinitropheno Mineralization. Nano, 2017, 12, 1750076.	0.5	16
67	Rapid removal of organic pollutants by a novel persulfate/brochantite system: Mechanism and implication. Journal of Colloid and Interface Science, 2021, 585, 400-407.	5.0	16
68	Reduced graphene oxide@TiO ₂ nanorod@reduced graphene oxide hybrid nanostructures for photoelectrochemical hydrogen production. Micro and Nano Letters, 2017, 12, 494-496.	0.6	10
69	Hydroxyalkylation of phenol to bisphenol F over heteropolyacid catalysts: The effect of catalyst acid strength on isomer distribution and kinetics. Journal of Colloid and Interface Science, 2016, 481, 75-81.	5.0	9
70	The Potential Strategies of ZnIn2S4-Based Photocatalysts for the Enhanced Hydrogen Evolution Reaction. Frontiers in Chemistry, 0, 10, .	1.8	4